ISSN 2712-0562
Sustainable Engineering and Innovation
Original Research
Vol. 6, No. 2, September 2024, pp.185-198
https://doi.org/10.37868/sei.v6i2.id344

Automatic human age estimation from face images using MLP and RBF neural network algorithms in secure communication networks

Haider TH. Salim ALRikabi[1], Ali Assad[1], Mohammed Jawad Al Dujaili[2], Ibtihal Razaq Niama ALRubeei[1]
[1]Electrical Engineering Department, College of Engineering, Wasit University, Wasit, Iraq
[2]Department of Electronic and Communication, Faculty of Engineering, University of Kufa, Najaf, Iraq

*Corresponding author E-mail: hdhiyab@uowasit.edu.iq

Received Jan. 5, 2024
Revised Aug. 07, 2024
Accepted Aug. 18, 2024

Abstract
Age estimation finds application in several contexts including biometric authentication, surveillance, forensic investigations, and the entertainment industries, among others, making it a realistic, complex, and relevant problem in the subfield of machine vision and pattern recognition. This article proposes a system that can determine the age of people by applying the multilayer perceptron neural network technique, feature fusion, and integration. It is imperative to define three fundamental stages of the proposed procedure. One of the methods necessary at the first stage involves face parts detection and resizing. The second activity is feature extraction of the facial regions of the video frames. To do this, we select and use features through the use of Gabor Filters, SIFT, and LBP with optimal values being picked through combinations. The third step in the process entails making an age range prediction of the face image using neural network algorithms such as MLP and RBF for securing communication networks. For further reduction of dimensions and for getting rid of any possibly overlapping features, independent component analysis (ICA) is used. The datasets adopted for this research work are FG-NET and PAL which are widely acclaimed research data sets. Simply based on the features adopted, the proposed age estimate procedure was seemingly superior to the MLP algorithm and possessed high accuracy for a given range of ages.

Keywords: Age estimation, Feature extraction, Feature selection, ICA, ANN, Communication networks

1. Introduction

The human face is truly teeming with a great number of different personal characteristics that help us identify individuals, determine their emotional state, and assess their sex, age, and race, if necessary. This data is being put to great use today by state-of-the-art face-based natural human-computer interaction systems that are training computers to recognize human faces and their body language. Among the concerns within this field, the estimation of human age is one of the fields that has not reached its conclusive discoveries. While some achievements have been made, there is still much that is yet to be explored regarding this innovative aspect of machine vision [1]. If you want to make your story and say, you do not know this man's age just by the face, then you have to be able to identify specific areas that are prone to show marks of aging. This technology has

recently emerged as a highly useful area of research since its versatility can be observed in various sectors including computerized customer contact management and security control and computer-based age estimation by facial recognition. As more and more people develop an interest in this particular field of study, scientists are now working hard to try and understand how to intensify these technologies to reach their full capabilities [2]. The methods employed in this discipline can generally be grouped into two types. One of them is the identification of ones that rely on the classification techniques and the identification of ones that rely on recognizing specific face characteristics. As for the age pre-estimations the characteristic approaches employ more generic age intervals and on the other hand, the categorization methods offer a higher level of age estimation. Numerical and qualitative research and studies in this area reveal that there are limitations and challenges in identifying people's ages, and this page has been designed to address such loopholes as much as possible. Local features, general features, and the combination of local and general features are distinct types of facial features [3-7].

When dealing with faces, the researchers take into account numerous aspects that include the number of layers in the face and the number of wrinkles specifically under the eyes and the forehead, skin color, texture, and the physiognomy of the face. Such regional details could be relevant, but they are not fully conclusive in every situation. The non-membranous features are more accurate at portraying attributes such as gender, skin color, and size and shape of the face. To get a fuller view of a person's look, researchers frequently use a mix of local and global information when creating age estimation methods. The continuous effort to enhance our capacity to predict age from facial features relies heavily on these composite traits. In order to get an approximate age, most people employ a mix of local and general features; naturally, the more precise and well-executed the feature extraction throughout the face, the more precise the age estimate will be [8-11].

Here, we offer a method for estimating people's ages using feature fusion and integration in conjunction with the multilayer perceptron neural network technique. Three primary procedures make up the suggested approach. Recognizing and resizing face regions is part of the initial pre-processing step. Step two is selecting critical facial features from various locations. Gabor Filters, SIFT, and LPB are some of the methods used to do this. After these characteristics are retrieved, we pick the ones that are most applicable and beneficial. Step three involves making an age range prediction for the face image using sophisticated algorithms such as RBF Neural Networks and MLP. Additionally, we use ICA to remove redundancy and decrease the dimensionality of our data, which guarantees accuracy and efficiency. We used the popular databases FG-NET and PAL to see how well our method worked. Please see Figure 1 for a graphical depiction of our procedure.

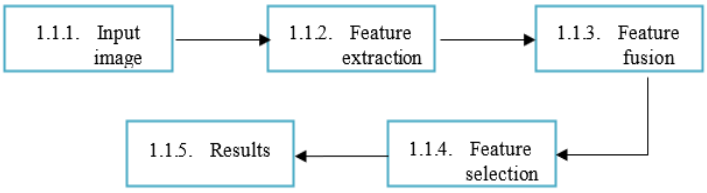

Figure 1. System overview

2. Related works

At different ages, people's faces can take on different patterns, and these patterns can change throughout time. While every person's face is unique, there is a standard set of characteristics that can be used to identify them [12]. An approach to face description is offered in [13] that makes use of a hierarchical feature extraction algorithm. There are two stages to extracting features for the age estimation approach. The initial stage involves the extraction of general features from the AAM model's shape and appearance parameters. The general shape and texture of the face can be discerned from these. Using Gabor filters to zero in on particular regions of the face, the second step is to extract skin and wrinkle features as local features. The most useful and informative qualities of a face for age estimate can be captured by combining these general and local features to generate a feature vector. The research forecasts are more accurate and reliable since this method provides a thorough and

detailed view of the face. This technique has a somewhat robust nature to the alterations that can be caused by variations in the angle and direction of the face due to the use of Gabor filters. They proposed the AGES system in [14] utilizing face photos from a set of individuals of different ages for recreating the aging effect. The AGES algorithm mentioned above is composed of two phases – learning and age estimation. Learners apply the principal component analysis (PCA) in the learning phase to define a subspace for the age model. This subspace is useful when trying to find features related to age estimates in order to make the estimate more accurate. Some of the machine vision applications that have exhibited promising values when implementing this method are biometrics, security and surveillance, and even arts. A new approach for estimating age from facial photos was recommended in [15] and involved the biologically inspired features (BIFs) method. Their method showed great promise for age estimate in machine vision, with remarkable results on both the FG-NET and YGA databases. Researchers point out in [16] that pictures of people's faces can reveal a lot about them, including their gender, personality traits, and even their approximate age, all with very little work. There have been a lot of studies on automatic ways to extract this information from face pictures because of the possible usefulness of this data in several contexts. Results in fields including customer relationship management, biometrics, security, and surveillance have been encouraging as a consequence of this.

There are two parts to the aging process that researchers suggest in their study [17]. The first part covers the years between birth and adulthood, when the head and face undergo substantial changes in size, and the second part covers the years between adulthood and aging. There have been advancements in this area despite the limitations, thanks to excellent tools for precisely analyzing face features to predict age. An approach to estimating age and determining gender is laid out in [1, 18]. A technique that enhances the face feature extraction stage; it is based on geometric characteristics and the principal component analysis (PCA) method. The picture database is partitioned into thirteen categories to assess this technique. Individuals within the same age bracket are given a weight vector in this particular database. In order to identify the face and determine the age range, a technique is provided in [19] that uses a triangular shape that is created by combining the eyes and mouth of an isosceles triangle.

3. The proposed method

Feature extraction and classification are the two main steps in most age estimation systems. There are essentially two stages to the procedure described in this study. The first step is to extract and fuse features, and then choose the best ones. The second step is to classify the features using a Neural Network using the test and training data from the first step. In the article's opening, the field operations of the two sections are discussed independently. The procedure of the suggested approach is illustrated in Figure 2.

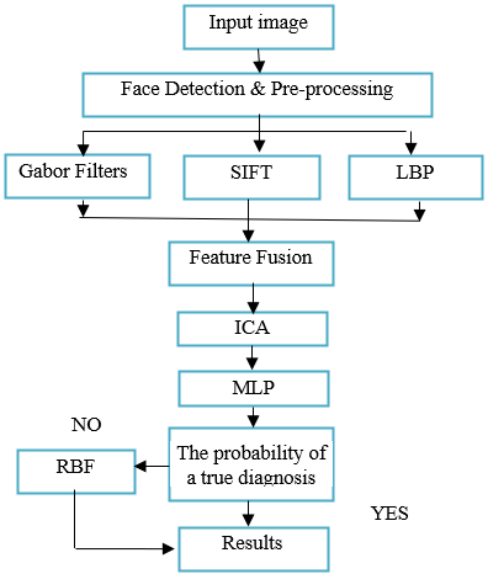

Figure 2. The proposed age estimation method

In the first stage, known as pre-processing, as shown in Figure 2, the 128 by 128-pixel region is shrunk after the face area in the input photos is recognized and cut. A set size for all the specified parts of the face is the goal of this endeavor. Step two involves using features from Gabor Filters, SIFT, and LBP, combining them, and then selecting the most appropriate features. Step three involves applying the RBF and MLP neural network algorithms to the face image to forecast its age range. In addition, ICA is used to get rid of duplicates and shrink dimensions. This research makes use of two popular datasets, FG-NET and PAL. The many phases of the process are illustrated in detail in Figure 2.

3.1. Pre-processing

During the pre-processing phase, the critical features of the facial image are recognized as key points. Subsequently, the surrounding regions are extracted as smaller images so that these points can be utilized. To do this, we extract five regions from the facial image: the eyes, nose, two regions surrounding the lips, and the rest. In the image, these sections are referred to as routes or sub-areas [20]. Using these procedures will make the proposed system more precise. Here is the pre-processing method illustrated in Figure 3.

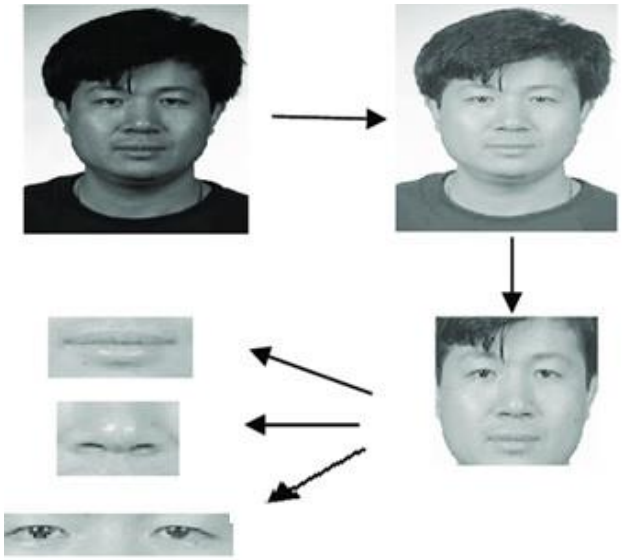

Figure 3. A view of the pre-processing process

3.2. Feature extraction

Choosing the right traits to describe the face is the first step in age estimation. Along with producing the most distinctive traits, these characteristics should include information that is insensitive to modifications like scale and rotation. In this research, we use a suggested technique to obtain a good facial representation from face photos by means of feature vector extraction. A combination of Gabor Filters, SIFT, and LBP features, with the right ones chosen after merging, is recommended. Then, using the features retrieved from the suggested approach, we apply the ICA dimension reduction method to the input vector in order to make vectors with the maximum resolution features while reducing their dimensions.

3.2.1. Gabor filters

Using matching graphs of coefficients acquired by Gabor filters is one of the successful ways for human age estimation (as indicated in [21]). By merging Gabor filters with Gabor wavelets, it is possible to extract information from previously unseen waves. The two-dimensional Gabor filter is the more common option, although the one-dimensional mode serves well as an intermediary filter for processing speech and other one-dimensional data. Detection and face area detection make heavy use of two-dimensional Gabor filters [22]. A combination of an exponential and a Gaussian function yields the Gabor filters depicted in Equation 1. We show that when comparing time-domain and signal-frequency-domain displays, the Gabor wavelet provides the best

correlation. Also, the time and frequency displays of these filters are identical. Each image-processing Gabor filter has its own unique frequency and direction, and the filters are two-dimensional [23].
Photographs of senior men or women with attractive features, or photographs of poor quality, tend to be textured delicately and lack smoothness. The delicate nature of these features makes feature extraction a formidable challenge; as a result, the Gabor filter, one of the most popular weave analysis methods, is employed to extract the feature from the targeted region of the face. Equation 1 represents the Gabor filter in its generic form.

$$"G(x,y,\theta,u,\sigma) = 1/\ 〚2\mu\sigma〛\ ^2\ exp\{(-(x^2 + y^2))/\ 〚2\sigma〛\ ^2\} * exp\{2xi(u\ x\ cos\theta + u\ y\ sin\theta\}" \quad (1)$$

The set of specific parameters for (θ, u, σ) is transformed into the discrete Gabor filter G^[x, y, θ, u, σ] shown in Equation 2 if the sine wave frequency, 1 = √ (-1) in the previous equation, θ is the function's controller, and σ is the standard deviation of the Gaussian coverage.

$$\widehat{G}[x,y,\theta,u,\sigma] = G[x,y,\theta,u,\sigma] - \frac{\sum_{j=-n}^{n}\sum_{j=-n}^{n} G[x,y,\theta,u,\sigma]}{(2n+1)^2} \quad (2)$$

In this regard $(2n + 1)^2$ indicates the size of the filter. The Gabor filter is canonized with face images and the results are stored in feature format. The results obtained from the Gabor filter are useful when the three parameters (θ, u, σ) are selected correctly. To get the right parameters, the results must be tested on the images several times.

3.2.2. SIFT

One of the most challenging problems in computer vision is the estimation of a person's age from facial photographs; this technique has many possible uses, from security to the entertainment industry. It might best approximate an individual's age which is one solution to this dilemma by subjecting the features extracted from the facial photos to a regression model [24]. Issues such as age estimate and other problems in computer vision real world have revealed that SIFT is among the most popular and frequently used feature extraction techniques. There are several approaches to detect objects in images and one of them is SIFT. Since its initiation by David Lowe in the year 1999, it has gained immense popularity for the purpose of item matching and recognition from different viewpoints. The SIFT algorithm identifies picture elements that are most relevant and does not change about size, orientation, and lighting of the picture. In the difference-of-Gaussian (DoG) scale space representation of the picture, the important features which are also called the key points are detected from the local maximum and the minimum. First, it is possible to take face pictures for the SIFT function in order to use SIFT for estimating the age. The next step that can be taken is to train a regression model so that it can link the features that were retrieved to age labels. Next, new face photographs can also undergo SIFT feature extraction and the age label of the face photographs can be estimated as per the trained model described above. This will help the algorithm to have a rough estimation of the age of the images. Finally, once the key points have been found, SIFT computes a descriptor for each key point that contains information about the orientation and scale of the picture at that location. To find suitable ages for facial photos, the descriptors are used to align key points between two or more images [25]. Some measures can be taken to simplify the SIFT algorithm's equation: A number of measures can be taken to simplify the SIFT algorithm's equation: Detection of primary extrema in the DoG scale space is the first step in scale-space extrema recovery. The presented image is convolved with a series of Gaussian kernels of different sizes. The difference between successive images in this series generates the DoG scale space. This part of the approach describes how the orientations are applied and how the key points are localized. This is done by fitting a quadratic function in the DoG scale space at each extremum point to detect the location and scale of each key point; the consequent invariance to image rotation. The notable feature of an image is termed the key point and the vector that sketches the nature of the local appearance of the image in its neighborhood corresponds to the key point descriptor. It is calculated from the gradient magnitude and the gradient direction of the pixels of the picture in a circular neighborhood of the key point. Following that, we employ a distance measure to match the key points of the two pictures, which could be the cosine

similarity measure or a simple distance measure such as the Euclidean distance. To determine the DoG pyramid, one can use the following equation: To determine the DoG pyramid, one can use the following equation:

$$D(x,y,\sigma) = (G(x,y,k\sigma) - G(x,y,\sigma)) * I(x,y) = L(x,y,k\sigma) - L(x,y,\sigma) \quad (3)$$

$$D(x,y,\sigma) = 1/(2\pi\sigma\text{^}2\ )\ \ e\text{^}(-((x\text{^}(2\ ) + y\text{^}2)/(2\sigma\text{^}2\ ))) \quad (4)$$

In this case, G(x,y,σ) stands for a standard deviation for the Gaussian filter function, and D(x,y,σ) is the value of the DoG picture at position (x, y) and scale σ. In the DoG pyramid, σ is the factor that decides the scale difference between two neighboring images at location (x, y). The default value for k is roughly 1.6. The original image's intensity value at coordinates (x, y) is denoted as I(x, y). Typically, a factor of 2 is used between each scale for computing the DoG images, and then these images are combined to form a DoG pyramid. The next step is to identify the image's critical points by looking for scale- and location-dependent local extrema in the DoG pictures. Afterward, a collection of SIFT descriptors is used to characterize these points. These descriptors are calculated based on gradient orientations and magnitudes in a local area surrounding each point, as shown in Equations 5 and 6.

$$M(x,y) = \sqrt{(\blacksquare(L(x+1,y)) - (x-1,y))\text{^}2 + @(L(x,y+1) - L(x,y-1))\text{^}2\ )} \quad (5)$$

$$\theta(x,y) = \ \llbracket tan \rrbracket\ \text{^}(-1)\ \ ((L(x,y+1) - L(x,y-1)))/(L(x+1,y)) - L(x-1,y))\ ) \quad (6)$$

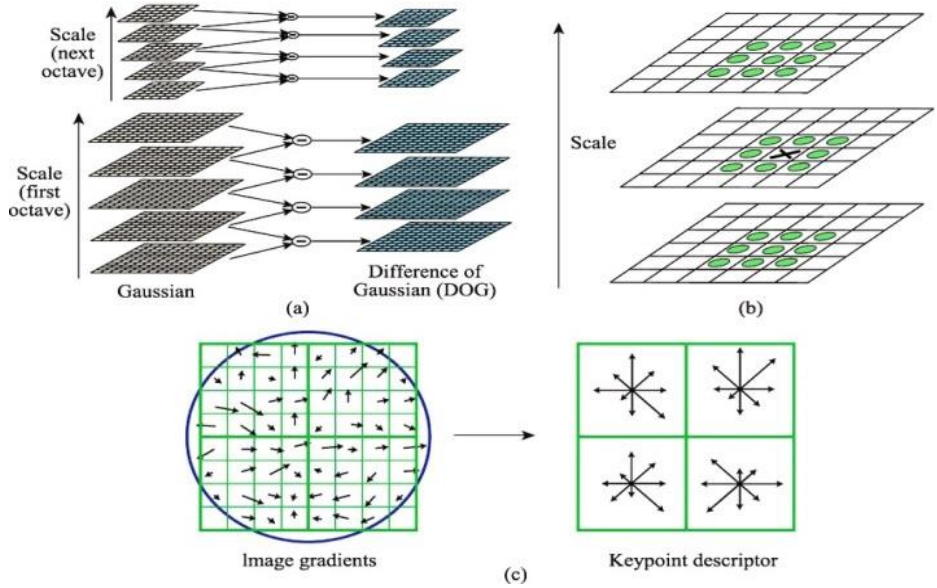

Figure 4. The elementary SIFT operator

3.2.3. LBP

LBP was developed by Ojala et al. [26] in 1996 to represent the image texture in a basic and efficient manner through the use of a texture descriptor. LBP stands for Local Binary Pattern which is concerned with the extraction of features from photos. In other words, LBP is a process in which every pixel in an image is compared to the pixels close to it and the outcome is converted into a binary code. In that case, if the sheer size of the neighboring pixel is dependent upon the size of the center pixel and is either smaller or larger than the center pixel it receives the value of 0 or 1 in binary scale. This process is repeated for each pixel in the image, but the scaled erroneously displaced pixel can contribute to the error as well. What is obtained in the end is an N-bit binary code where N shows the number of neighboring pixels used for the comparison. It is considered that it is possible to either for each pixel in the picture to calculate the LBP descriptor or interpret the new picture where the LBP codes will be in the place of the initial pixels. Indeed, a set of LBP codes can be used as a

characteristics list for different computer vision tasks like picture classification, object recognition, face recognition, etc. It is also important to mention that the LBP texture descriptor has several advantages over other possible descriptors such as simplicity of interpretation, fast computational time, and being relatively invariable to the changes in illumination [27]. Substituting the number of distinct neighborhoods into Equation 7 above yields the LBP code.

$$〖LBP〗_{(P,R)} = \sum_{(P = 0)^{(P-1)}} 〖S(g_p〗 - g_c)2^p \quad (7)$$

Where g_c stands for the intensity value of the central pixel, g_p stands for the intensity of the neighboring pixel with index p which stands for the total number of involved neighbors and R stands for the radius of the neighborhood.

The function S can be expressed as:

$$S(x) = \begin{cases} 1 & if\ x \geq 0 \\ 0 & if\ x < 0 \end{cases} \quad (8)$$

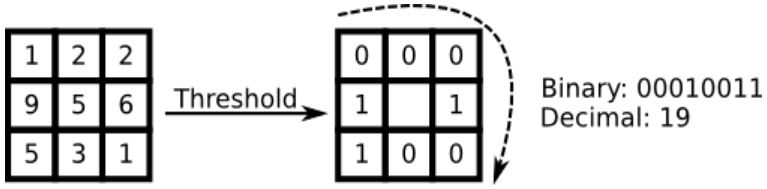

Figure 5. The basic LBP operator

3.3. Fusion and feature selection

Local features in areas like the forehead, under the eyes, and cheeks, as well as general traits like the face's structure and shape, are frequently utilized. To improve the precision of age estimation systems that operate automatically, this study suggests a new method that integrates Gabor filters, SIFT, and LBP.

3.4. Reducing the dimensions of features

Selecting relevant characteristics and discarding irrelevant ones is the next step after feature extraction. To improve recovery accuracy and speed, the suggested method eliminates the unnecessary frequency components taken from the image. Feature spaces of two individuals or a person's image in various states have been the subject of a great deal of research. These analyses revealed that low frequencies have a larger role than high frequencies in the suggested technique. The image's texture, which is close to one another in various persons, is indicated by high frequencies. The low frequencies, on the other hand, are affected by the size and placement of the various facial features, which vary from person to person. An effective technique in the area of non-beneficial feature reduction, independent component analysis (ICA) has been utilized in our suggested approach. Mrs. Bartlett first suggested this technique for identifying people from photographs of their faces in 1998 [28]. Because it is more expressive and takes higher-order moments into account, the ICA technique outperforms the Eigenface method in terms of identification rate. This is in contrast to the PCA method. After calculating the eigenvectors using the PCA approach and whitening and dimensionally reducing the data, we proceed to calculate the transfer vectors. This is because, as per the investigations, the ICA method performs better on whitened and reduced data [29].

3.5. Classifications

Face identification, feature extraction, and age estimation are the three phases involved in automatic age estimation, as previously stated. Finding and removing the face area from the input picture is the initial step in utilizing a face detector. Step two is applying several image processing methods to the facial area in order to extract characteristics like shape, texture, and wrinkles. Step three involves using an age estimation model to

extrapolate a person's age from their collected characteristics. There are two hierarchical approaches and one single-stage method for learning the age estimation function. In single-step mode, a classifier estimates the age and then chooses the desired image's age tag from the pool of all available tags. When it comes to estimating ages, however, the hierarchical technique makes use of many classifiers. Neural networks such as RBF and MLP are utilized in this piece.

3.5.1. MLP

An input layer, a hidden layer (or layers), and an output layer make up a multi-layer perceptron (MLP) neural network [30, 31]. With the exception of the input layer, all of the other layers' neurons are independent compression functions with biases and can execute addition operations. In order to obtain the target average total error value, the number of hidden layers and neurons in each layer are often selected through trial and error approaches, rather than being predetermined [32]. For the input sample, the total squared error for all nodes in the network's output layers is computed:

$$E\_P = 1/2\ (d\hat{}p - y\hat{}p\ )\hat{}2 = 1/2 \sum\_(j = 1)\hat{}s \blacksquare [\![(d\_j\hat{}p - y\_j\hat{}p)]\!]\hat{}2 \quad (9)$$

The order of the desired output vector is denoted as d^p, and the actual output vector is represented by y^p. Similarly, the desired output for the j^{th} node of the output layer is represented by d_j^p, and the actual output is denoted by y_j^p. The size of the output vector is represented by s. Based on these values; the sum of squared error can be calculated for a sample of P patterns in the following manner:

$$E\_P = \sum\_(p = 1)\hat{}p \blacksquare E\_P\ = 1/2 \sum\_(P = 1)\hat{}P \blacksquare \sum\_(J = 1)\hat{}S \blacksquare [\![(d\_j\hat{}p - y\_j\hat{}p)]\!]\hat{}2 \quad (10)$$

To reduce the error rate E, the weights are updated according to the following equation.

$$W\_ij\ (t + 1) = W\_ij\ (t) + \eta \times \Delta W\_ij\ (t) + \alpha \times \Delta W\_ij\ (t - 1) \quad (11)$$

$$\Delta W\_ij\ (t) = -(\ [\![\partial E]\!]\ \_P\ /(\ [\![\partial sw]\!]\ \_ij\ (t))) \quad (12)$$

Iteratively adjusting the weight of the edges between neurons is required to train an MLP neural network. In this procedure, the variables η and α regulate the learning rate. At time t, Wij(t) represents the weight of the edge connecting nodes i and j, and at time t+1, Wij(t+1) represents the weight of the same edge. After a certain number of iterations or when the error rate drops below a certain threshold, the learning process stops. Figure 6 shows the architecture of a multi-layer perceptron neural network.

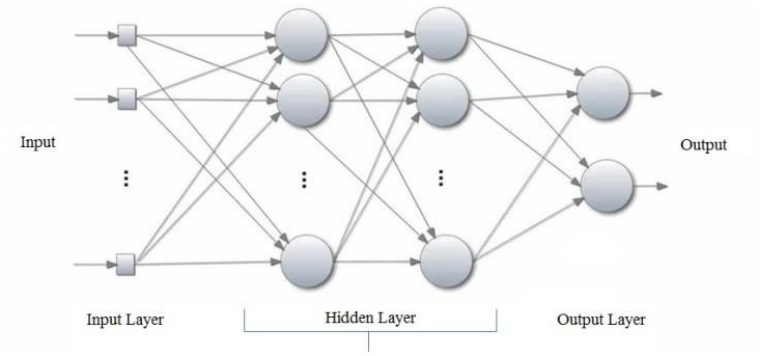

Figure 6. MLP neural network structure

3.5.2. RBF

Among the many applications of artificial neural networks, RBF neural networks are particularly well-suited for function approximation, classification, and clustering due to their use of radial basis functions as activation functions. The input, hidden, and output layers make up the architecture of a Recurrent Binary Flow (RBF) neural network [33]. Following feature extraction from the face area, the input layer gets the features, and the hidden layer transforms them using a nonlinear function. The output layer concludes by estimating the person's age. The input layer of an RBF neural network is linked to a hidden layer that contains a collection of radial basis functions. These functions are responsible for converting the input into a feature space with higher dimensions. This information is then used by the output layer to generate the appropriate values. A huge dataset of face photos along with their ages is used to train the RBF neural network model. This dataset teaches the model the relationship between age and facial traits. After training, the model reliably estimates the age of an unlabeled facial picture. The amount and variety of the training dataset, along with the quality of the face identification and feature extraction procedures, determine the age estimate model's accuracy. More accurate age predictions than linear regression models can be achieved by training RBF neural networks to learn nonlinear correlations between facial characteristics and age [33]. See Figure 7 for a representation of an RBF neural network's architecture.

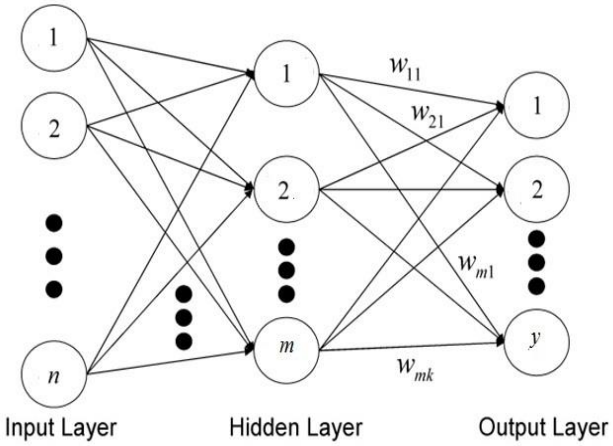

Figure 7. RBF neural network structure

The activation function of RBF units is expressed as Equation 13.

$$R\_i\ (x) = R\_i\ (\|x - c\_i\ \|/\sigma\_i\ ) \quad i = 1,2,\ldots,m \tag{13}$$

In an RBF neural network, a collection of n-dimensional vectors called the centers of the RBF units (c_i) modify the input feature vector x. The width parameter σ_i, which determines the activation function range, is likewise present in each RBF unit. The symbol m stands for the quantity of RBF units. The Gaussian function, with its mean vector ci and variance vector σ_i, and its expression in Equation 14 is a popular option for the activation function of RBF units.

$$R\_i\ (x) = exp(\|x - c\_i\ \|\text{^}2/\ \llbracket\sigma\_i\rrbracket\text{^}2\ ) \tag{14}$$

The output units are linear and therefore the response k will be the output unit for input x in the form of Equation 15.

$$y\_i\ (x) = \sum\_(i = 1)\hat{}m \blacksquare \ \llbracket R\_i\ (x)\ \ w\_mk\ \rrbracket \quad (15)$$

w_mk = the weight of the i-th connection from the RBF unit to the j-th unit of the output layer.

Compared to other neural network architectures, RBF neural networks are relatively simple and fast to train. They can also be used to approximate any continuous function to arbitrary accuracy, given enough hidden units. However, choosing the appropriate number and placement of the radial basis functions can be challenging, and the resulting network may be sensitive to the choice of initial parameters.

4. Experimental results

In this research, the mean absolute error was used. As its name suggests, MAE is the difference between the average age predicted and the actual age and can be calculated by Equation 16:

$$MAE = \frac{\sum_{i=0}^{n} |E_{Ai} - R_{Ai}|}{n} \quad (16)$$

Inside the range of n examined samples, where E_{Ai} denotes the estimated age and R_{Ai} denotes the actual age. Two well-known datasets, FG-NET and PAL, were utilized to assess the suggested approach in this research, bearing in mind that the quantity of training data significantly impacts the model's accuracy. One such age database is FG-NET, which is open to the public. The 82 individuals represented here represent a wide range of racial and ethnic backgrounds, and the 1002 high-resolution color or greyscale face photographs capture a wide range of expressions, lighting, and poses. With an average of twelve images per person, the ages vary from zero to ninety-six, and the photos are organized chronologically [34]. We used 157 jpg images from the PAL database, which has a resolution of 646 × 480. In this database, the photos are sorted into four age groups: 18–29, 30–49, 50–69, and 70–94 years old [35]. Twenty percent of the photos in each database were utilized for testing purposes, while the remaining portion was employed for training the models. In order to save processing time and avoid computational overhead caused by extraneous information in the image, like the border and background, all of the images used for each stage of model building and testing are first converted to a greyscale model. Then, the inner portion of the face is extracted. It has a dimension of 128*128 and is separated from the image.

Various experiments have been conducted to assess the suggested model's performance and interpret the results. In terms of determining people's ages from face photos, the test results demonstrate that the suggested model is accurate and has practical application. Here we'll go into the specifics of the implementation and the testing. Tables 1 and 2 show that when RBF and MLP Algorithms are applied to the FG-NET database, the Gabor filters approach achieves a greater percentage accuracy than the SIFT method. Gabor filters for comparison graphs of calculated coefficients provide the basis of a highly effective approach for estimating human age. The SIFT method outperforms the LBP method in terms of accuracy percentage as well. The LBP approach outperforms Gabor filters and SIFT in terms of accuracy, and the gap between the three is negligible. In comparison to SIFT and LBP, the Gabor filters technique performed very well. Compared to using Gabor filters, SIFT, and LBP independently, combining them yields better results. Another effective combination is Gabor filters+ LBP. Figure 8 displays the top outcomes from the FG-NET database across several age categories. Tables 3 and 4 show that compared to the Gabor filter approach, the SIFT method achieves a better percentage of accuracy when using the PAL database in conjunction with RBF and MLP algorithms. The Gabor filters approach outperforms the LBP method in terms of accuracy percentage as well. The LBP approach outperforms Gabor filters and SIFT in terms of accuracy, and the gap between the three is negligible. Instead of using Gabor filters, SIFT, and LBP independently, combining them yields better results. At last, the most effective strategy is the combination of Gabor filters, SIFT, and LBP. Figure 9 displays the top findings found in the PAL database for various age groups. While the MLP Algorithm performed adequately, the RBF Algorithm outperformed it. Results also showed a significant improvement when the ICA approach was used.

Table 1. Percentage accuracy in four age groups for FG-NET database with MLP classification

Age groups	Gabor	SIFT	LBP	Gabor+ SIFT	Gabor+ LBP	SIFT+ LBP	Gabor+ SIFT+ LBP
0-25	95.4	95.1	94.8	97.3	96.1	95.7	98.4
26-45	95.2	94.7	94.3	97.8	96.4	96.2	98.2
46-70	95.8	95.5	94,1	96.9	96.2	96.9	98.7
71-96	95.8	95.6	94.6	96.8	96.4	96.1	98.1

Table 2. Percentage accuracy in four age groups for FG-NET database with RBF classification

Age groups	Gabor	SIFT	LBP	Gabor+ SIFT	Gabor+ LBP	SIFT+ LBP	Gabor+ SIFT+ LBP
0-25	96.4	95.9	95.5	97.8	97.1	96.7	99.4
26-45	95.8	95.7	95.3	98.4	97.4	96..5	99..2
46-70	96.2	95.9	95,7	97.7	96.8	97.5	99.5
71-96	96.5	96.2	95.4	97.5	96.9	96.7	99.1

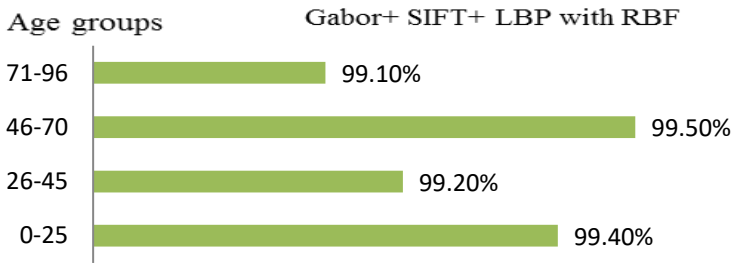

Figure 8. The best results that were obtained in a database FG-NET for different age groups

Table 3. Percentage accuracy in four age groups for PAL database with MLP classification

Age groups	Gabor	SIFT	LBP	Gabor+ SIFT	Gabor+ LBP	SIFT+ LBP	Gabor+ SIFT+ LBP
0-25	95.2	96.3	93.1	95.9	97.2	98.2	98.7
26-45	95.4	95.8	93.6	95.8	95.4	98.7	99.1
46-70	94.7	95,1	93.5	96.1	96.8	98.4	98.9
71-93	94.4	94.6	94.1	95.4	96,2	98.8	99.1

Table 4. Percentage accuracy in four age groups for PAL database with RBF classification

Age groups	Gabor	SIFT	LBP	Gabor+ SIFT	Gabor+ LBP	SIFT+ LBP	Gabor+ SIFT+ LBP
0-25	95.2	96.3	93.1	95.9	97.2	98.2	99.3
26-45	95.4	95.8	93.6	95.8	95.4	98.7	99.5
46-70	94.7	95,1	93.5	96.1	96.8	98.4	99.2
71-93	94.4	94.6	94.1	95.4	96.2	98.8	99.6

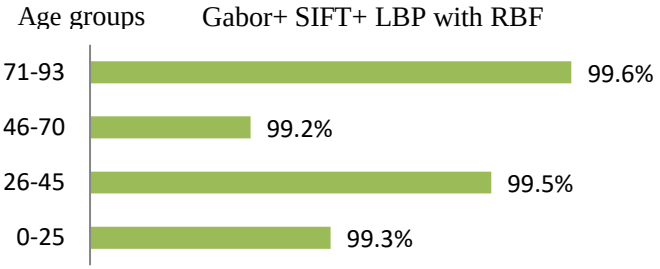

Figure 9. The best results were obtained in a database PAL for different age groups

The intersection of microstrip devices and automatic human age estimation through neural networks offers innovative solutions for enhancing security in communication networks [36-39]. By leveraging the strengths of both technologies, it is possible to create robust systems that ensure secure access while utilizing advanced

biometric analysis for user verification [40-43]. The efficiency of microstrip devices allows for real-time data transmission, which is crucial for applications requiring immediate feedback, such as security systems that assess individuals before granting access [44-47].

5. Conclusion

When trying to determine an individual's age from a photograph of their face, most people look at the overall look of the face in addition to the collection of fine and coarse features in various areas of the face. To determine the approximate age range of a face image, this article employs a combination of Gabor filters, SIFT, and LBP features, merges and selects the most relevant features from each, and then applies the MLP and RBF neural network algorithms. It is also possible to minimize dimensions and remove redundancy by using ICA. The accuracy of the age prediction is directly proportional to the quality and precision of the feature extraction across the various facial regions. Since the accuracy of such systems is heavily dependent on the feature selection extraction stage, it was noted that this stage is particularly important in the automatic process of age estimation from face images. Execution results on the benchmark face images demonstrated that the combined approaches outperformed the individual ones. When applied to the pictures of two well-known databases, FG-NET and PAL, the given method outperformed previous methods on both datasets.

Conflict of interest

The authors declare that they have no conflict of interest and all of the authors agree to publish this paper under academic ethics.

Author contributions

Haider TH. Salim ALRikabi and Ali Assad conceptualized and designed the study. Mohammed Jawad Al Dujaili developed the algorithms and conducted the experiments. Ibtihal Razaq Niama ALRubeei performed data analysis and interpretation. All authors contributed to writing and reviewing the manuscript, with Haider TH. Salim ALRikabi as the corresponding author.

References

[1] H. Han, C. Otto, and A. K. Jain, "Age estimation from face images: Human vs. machine performance," in *2013 international conference on biometrics (ICB)*, 2013: IEEE, pp. 1-8.

[2] X. Geng, Z.-H. Zhou, Y. Zhang, G. Li, and H. Dai, "Learning from facial aging patterns for automatic age estimation," in *Proceedings of the 14th ACM international conference on Multimedia*, 2006, pp. 307-316.

[3] C.-T. Lin, D.-L. Li, J.-H. Lai, M.-F. Han, and J.-Y. Chang, "Automatic age estimation system for face images," *International Journal of Advanced Robotic Systems*, vol. 9, no. 5, p. 216, 2012.

[4] R. Jana and A. Basu, "Automatic age estimation from face image," in *2017 International Conference on Innovative Mechanisms for Industry Applications (ICIMIA)*, 2017: IEEE, pp. 87-90.

[5] R. a. M. Al_airaji, and I. A. Aljazaery, "Watermark Hiding in HDR image based on Visual Saliency and Tucker decomposition," *Karbala International Journal of Modern Science*, vol. 9, no. 3, p. 6, 2023.

[6] R. a. M. Al_airaji, and R. Kamil, "Classification and removal of hazy images based on a transmission fusion strategy using the Alexnet network," *Karbala International Journal of Modern Science*, vol. 10, no. 2, p. 14, 2024.

[7] H. T. Hazim, "A Novel Method of Invisible Video Watermarking Based on Index Mapping and Hybrid DWT-DCT," *International Journal of Online and Biomedical Engineering(iJOE)*, vol. 19, no. 04, pp. 155-173, 2023.

[8] G. Antipov, M. Baccouche, S.-A. Berrani, and J.-L. Dugelay, "Apparent age estimation from face images combining general and children-specialized deep learning models," in *Proceedings of the IEEE conference on computer vision and pattern recognition workshops*, 2016, pp. 96-104.

[9] R. Angulu, J. R. Tapamo, and A. O. Adewumi, "Age estimation via face images: a survey," *EURASIP Journal on Image and Video Processing*, vol. 2018, no. 1, pp. 1-35, 2018.

[10]I. A. Aljazaery, J. S. Qateef, A. H. M. Alaidi, and R. a. M. Al_airaji, "Face Patterns Analysis and Recognition System Based on Quantum Neural Network QNN," *International Journal of Interactive Mobile Technologies*, vol. 16, no. 8, 2022.

[11] H. T. S ALRikabi, "Secured Transfer and Storage Image Data for Cloud Communications," *international Journal of Online and Biomedical Engineering*, vol. 19, no. 06, 2023.

[12] A. S. Al-Shannaq and L. A. Elrefaei, "Comprehensive analysis of the literature for age estimation from facial images," *IEEE Access*, vol. 7, pp. 93229-93249, 2019.

[13] S. E. Choi, Y. J. Lee, S. J. Lee, K. R. Park, and J. Kim, "Age estimation using a hierarchical classifier based on global and local facial features," *Pattern recognition*, vol. 44, no. 6, pp. 1262-1281, 2011.

[14] X. Geng, Z.-H. Zhou, and K. Smith-Miles, "Automatic age estimation based on facial aging patterns," *IEEE Transactions on pattern analysis and machine intelligence*, vol. 29, no. 12, pp. 2234-2240, 2007.

[15] G. Guo, G. Mu, Y. Fu, and T. S. Huang, "Human age estimation using bio-inspired features," in *2009 IEEE conference on computer vision and pattern recognition*, 2009: IEEE, pp. 112-119.

[16] T. Bagh *et al.*, "Age estimation using Cameriere's seven teeth method with Indian specific formula in south Indian children," *Int J Adv Health Sci*, vol. 1, no. 2, pp. 2-10, 2014.

[17] A. Kamra and S. Gupta, "Automatic Age Estimation Through Human Face: A Survey," in *3rd International Conference on Electrical, Electronics, Engineering Trends, Communication, Optimization and Sciences*, 2016.

[18] N. K. abed, and I. R. N. ALRubeei, "Gender Recognition of Human from Face Images Using Multi-class Support Vector Machine (SVM) Classifiers," *International Journal of Interactive Mobile Technologies (iJIM)* vol. 17, no. 08, 2023.

[19] K.-H. Liu, S. Yan, and C.-C. J. Kuo, "Age estimation via grouping and decision fusion," *IEEE Transactions on Information Forensics and Security*, vol. 10, no. 11, pp. 2408-2423, 2015.

[20] X. Liu, Y. Zou, H. Kuang, and X. Ma, "Face image age estimation based on data augmentation and lightweight convolutional neural network," *Symmetry*, vol. 12, no. 1, p. 146, 2020.

[21] J. Kim, D. Han, S. Sohn, and J. Kim, "Facial age estimation via extended curvature Gabor filter," in *2015 IEEE international conference on image processing (ICIP)*, 2015: IEEE, pp. 1165-1169.

[22] G. Trivedi and N. N. Pise, "Gender classification and age estimation using neural networks: a survey," *International Journal of Computer Applications*, vol. 975, p. 8887, 2020.

[23] A. Othmani, A. R. Taleb, H. Abdelkawy, and A. Hadid, "Age estimation from faces using deep learning: A comparative analysis," *Computer Vision and Image Understanding*, vol. 196, p. 102961, 2020.

[24] D. G. Lowe, "Object recognition from local scale-invariant features," in *Proceedings of the seventh IEEE international conference on computer vision*, 1999, vol. 2: Ieee, pp. 1150-1157.

[25] M. M. Sawant and K. Bhurchandi, "Hierarchical facial age estimation using Gaussian process regression," *IEEE Access*, vol. 7, pp. 9142-9152, 2019.

[26] T. Ojala, M. Pietikäinen, and D. Harwood, "A comparative study of texture measures with classification based on featured distributions," *Pattern recognition*, vol. 29, no. 1, pp. 51-59, 1996.

[27] A. Singh and H. Pal Thethi, "Age Estimation from Face Images Using CNN Based on LBPH/LBP," in *ICT Infrastructure and Computing: Proceedings of ICT4SD 2022*: Springer, 2022, pp. 357-367.

[28] M. S. Bartlett and M. S. Bartlett, "Independent component representations for face recognition," *Face Image Analysis by Unsupervised Learning*, pp. 39-67, 2001.

[29] F. R. Bach and M. I. Jordan, "Kernel independent component analysis," *Journal of machine learning research*, vol. 3, no. Jul, pp. 1-48, 2002.

[30] O. Oladipo, E. O. Omidiora, and V. C. Osamor, "A novel genetic-artificial neural network based age estimation system," *Scientific Reports*, vol. 12, no. 1, p. 19290, 2022.

[31] R. K. Tiwari, "Human age estimation using machine learning techniques," *International Journal of Electronics Engineering and Applications*, vol. 8, no. 1, pp. 01-09, 2020.

[32] M. K. Benkaddour, "CNN based features extraction for age estimation and gender classification," *Informatica*, vol. 45, no. 5, 2021.

[33] M. J. Er, S. Wu, J. Lu, and H. L. Toh, "Face recognition with radial basis function (RBF) neural networks," *IEEE transactions on neural networks*, vol. 13, no. 3, pp. 697-710, 2002.

[34] Y. Fu, T. M. Hospedales, T. Xiang, S. Gong, and Y. Yao, "Interestingness prediction by robust learning to rank," in *European conference on computer vision*, 2014: Springer, pp. 488-503.

[35] Y. Fu, G. Guo, and T. S. Huang, "Age synthesis and estimation via faces: A survey," *IEEE transactions on pattern analysis and machine intelligence*, vol. 32, no. 11, pp. 1955-1976, 2010.

[36] M. S. Jameel, Y. S. Mezaal, and D. C. Atilla, "Miniaturized coplanar waveguide-fed UWB Antenna for wireless applications," *Symmetry*, vol. 15, no. 3, p. 633, 2023.

[37] A. R. Azeez, "UWB tapered-slot patch antenna with reconfigurable dual band-notches characteristics," *J. Mech. Contin. Math. Sci*, vol. 19, no. 3, 2024.

[38] Y. S. Mezaal and S. F. Abdulkareem, "New microstrip antenna based on quasi-fractal geometry for recent wireless systems," in *2018 26th Signal Processing and Communications Applications Conference (SIU)*, 2018: IEEE, pp. 1-4.

[39] F. Abayaje, S. A. Hashem, H. S. Obaid, Y. S. Mezaal, S. K. J. P. o. E. Khaleel, and N. Sciences, "A miniaturization of the UWB monopole antenna for wireless baseband transmission," vol. 8, no. 1, pp. 256-262, 2020.

[40] J. Ali and Y. Miz'el, "A new miniature Peano fractal-based bandpass filter design with 2nd harmonic suppression 3rd IEEE International Symposium on Microwave," *Antenna, Propagation and EMC Technologies for Wireless Communications, Beijing, China*, 2009.

[41] N. A. Hussien, A. A. Daleh Al-Magsoosi, H. T. AlRikabi, and F. T. J. I. J. o. I. M. T. Abed, "Monitoring the Consumption of Electrical Energy Based on the Internet of Things Applications," vol. 15, no. 7, 2021.

[42] Y. S. Mezaal, H. H. Saleh, and H. Al-Saedi, "New compact microstrip filters based on quasi fractal resonator," *Advanced Electromagnetics*, vol. 7, no. 4, pp. 93-102, 2018.

[43] H. A. Hussein, Y. S. Mezaal, and B. M. Alameri, "Miniaturized microstrip diplexer based on fr4 substrate for wireless communications," *Elektronika Ir Elektrotechnika*, vol. 27, no. 5, pp. 34-40, 2021.

[44] S. Roshani *et al.*, "Design of a compact quad-channel microstrip diplexer for L and S band applications," *Micromachines*, vol. 14, no. 3, p. 553, 2023.

[45] S. Roshani, S. I. Yahya, B. M. Alameri, Y. S. Mezaal, L. W. Liu, and S. Roshani, "Filtering power divider design using resonant LC branches for 5G low-band applications," *Sustainability*, vol. 14, no. 19, p. 12291, 2022.

[46] K. M. Tarrad *et al.*, "Cybercrime Challenges in Iraqi Academia: Creating Digital Awareness for Preventing Cybercrimes," *International Journal of Cyber Criminology*, vol. 16, no. 2, pp. 15–31-15–31, 2022.

[47] S. A. AbdulAmeer *et al.*, "Cyber Security Readiness in Iraq: Role of the Human Rights Activists," *International Journal of Cyber Criminology*, vol. 16, no. 2, pp. 1–14-1–14, 2022.